

# Technical Report: Fast Robot Arm Inverse Kinematics and Path Planning Under Complex Obstacle Constraint

David W. Arathorn

Dept of Electrical and Computer Engineering, Montana State University.

[dwa@giclab.com](mailto:dwa@giclab.com), [dwa@cns.montana.edu](mailto:dwa@cns.montana.edu)

Copyright 2019©David W. Arathorn

## Abstract

Described here is a simple, reliable method for rapid computation of robot arm inverse kinematic solutions and motion path plans in the presence of complex obstructions. The method is based on a restricted form of the MSC (map-seeking circuit) algorithm, optimized to exploit the characteristics of practical arm configurations. MSC representation naturally incorporates both arm and obstacle geometries. The consequent performance on modern hardware is suitable for applications requiring real-time response. On high-end GPGPU hardware computation of both final pose for an 8 DOF arm and a smooth obstacle-avoiding motion path to that pose takes approximately 200msec.

## Introduction

The term “inverse kinematics” as applied to robotic arm manipulators denotes the problem of determining the angles of each of the joints which, given a root position in 3-space, will locate the distal end of the last arm segment (or end effector) at a specified location in 3-space. There is a widely used method for solving inverse kinematic (IK) problems of this sort, which, for the audience of this paper, need not be described here. A limitation of this method is that when the IK problem needs to be solved for an arm operating in the presence of complex obstacles, the process of solution becomes awkward and computationally very expensive. Methods in the latter category will not be discussed here because the method described here derives from completely different origins. The underlying principle is that for clean solution of an inverse problem under constraints the representation has to naturally incorporate those constraints, no matter how complex they may be in practice.

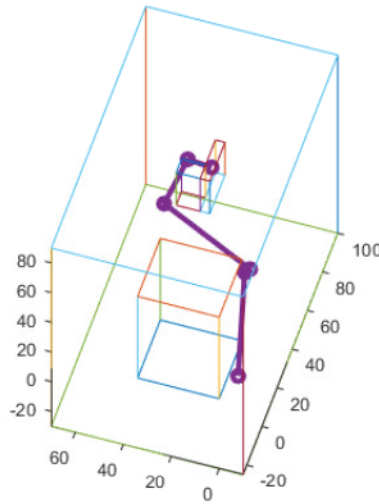


**Fig 1: 8DOF Arm “Reach Pose” Solution Amid Obstacles (shown as blocks)**

The practical use of robotic arms requires not only the solution of the articulation which will bring its working end to the target (we will refer to this articulation as the “reach pose”, Fig 1), it also requires a path of motion that takes it from its starting articulation to the reach pose. When operating in the presence of obstacles, determining this motion requires solving for a smooth sequence of articulations also constrained by the same obstacles.

This technical paper describes a method which, relying on a technique originating in another computational domain, gracefully and quickly solves the full problem described above: IK for both the reach pose and the motion path in the presence of arbitrarily complex obstacles. The method, when deployed on modern parallel computational hardware, can solve the full path planning and reach problem for an 8 degree-of-freedom arm, in a couple of hundred milliseconds. This speed allows accommodation of the arm to dynamic as well as static obstacles.

The method invoked for this purpose is a variant of the MSC (map-seeking circuit) algorithm [1]. MSC is a method for solving inverse problems which can be posed as a composition of transformations. The conventional MSC variant has been used extensively for machine vision, in which recognizing or interpreting the image of an object involves determining the sequence of visual transformations which map the image to a 3-D representation or model of the object. The conventional form of MSC can also be applied to IK problems. For robotic arms, the sequence of transformations (in effect, translations) to be determined are the sequence of mappings that take the root to the distal location of the first arm segment, the latter location to the distal location of the next arm segment, and so forth until the last transformation takes the proximal location of the last segment (or end effector) to the location of the target. The variant version of MSC described here solves the same problem, using a very similar representation, but exploits the specific characteristics of the arm IK problem for computational efficiency.

The means by which conventional MSC obtains its computational efficiency is by formation of superpositions of transforms and the “collapsing” of these superpositions by iterative convergence.

The variant described here, while using essentially the same representation of the problem, bypasses the method of solution of the conventional form for a much more readily understood highly pruned search. For those interested in the more general, conventional form of MSC, references are provided in the Appendices. These are not necessary for understanding the present variant.

A particular virtue of both the conventional and variant versions of MSC for the extended IK problem described in the opening is that the representation is entirely spatial and allows representation of the arm, its location in space, the target location and orientation in space, and all the obstacles in the environment. And the method of solution incorporates all of these concurrently.

### **The representations of the arm and obstacles**

MSC is a selection process. It selects a sequence of discreet transformations from sets of families of transformations, such that the composition of the selected sequence of mappings transforms one input parameter to another input parameter. The parameters may be thought of as variables or patterns. In conventional MSC the parameters are vectors representing space, and the mappings move the elements of the vectors in prescribed ways corresponding to geometric transformations. So, in a conventional MSC, the root location of the arm and its target would both be represented as a single non-zero element in a 3 dimensional array, and the MSC would determine a sequence of mappings which move the non-zero element in stages through 3-space to the target location. Of course this is a discretized representation of the IK problem: both space and the mappings must be discretized, so the solution is approximate. In this representation it is easy to see how obstacles can be represented in the same form. In a 3d array of the same dimensions as those which represent the arm segment endpoint locations, all the space occupied by obstacles is designated by a particular value, say zero, and all the free space is designated by another value, say 1. This 3d obstacle array can then be used as a mask to block any solutions which locate an arm segment in the voxels occupied by the obstacles.

The voxel representation of obstacles allows capture of obstacles in real-time by cameras that produce depth images. For reasons that will become apparent, obstacle volumes need not be filled. Dilation of the “skin” of obstacles, as captured by depth cameras, to a thickness greater than the sampling or waypoint interval, to be discussed later, suffices. However, obstacle capture is outside the scope of this discussion.

In conventional MSC as applied to IK, the mappings which represent arm segment positions are computed numerically from the coordinates of the spatial representation and then rounded back into the spatial representation just described for each step of the solution. (This derives from the machine vision application in which the array representation must be preserved for images.) In the variant MSC to be described here, arm locations remain represented numerically, while obstacles are represented spatially, as voxels, as just described, and the method maps between the two representations on the fly to achieve the same masking as described above. Despite the numerical representation, the process *mostly* remains a selection among discrete mappings. The “*mostly*” is significant. The difference, as will be seen, allows the variant MSC method to compute exact IK solutions despite discretizations of the mappings. For reasons related to “mostly” this variant is termed a “gap MSC” or gMSC.

## Discretization of the segment articulations

It has been found from experience that the best discretization for MSC of any 2DOF rotation is a so-called “tiling of the sphere.” The objective is to obtain a set of unit vectors from the origin which touch a sphere such that the sampling density of the sphere surface is approximately constant.

One way to accomplish this is to subdivide the equator into  $n$  divisions of azimuth, and use the great circle distance (or an approximation) between divisions along the equator as the approximate spacing for all the other latitudes. This results in decreasing numbers of generated vectors as the poles are approached. The elevation angles, or longitudes, are equidistant, as usual. The angle information is discarded, but the addressing of the vector set is by two indices: [elevation order, azimuth order], with a different number of azimuth indices for each elevation. The result is a *quiver* of unit vectors from the sphere center to the points on the sphere surface of approximately uniform density.

A single quiver is used to establish the joint rotation choices for the first and second and fourth (if necessary) segments’ articulation mappings, and the mappings themselves are simply the quiver unit vectors  $\mathbf{q}_{i,j}$  multiplied by the segment length  $l_s$  and restricted to some subset by other constraints. In practice elevation and equatorial azimuth angles of 2 or 1 degree have proven effective, though smaller angle increments can be used at the cost of compute time. The quiver also has the side benefit of limiting the number of equivalent solutions in the obstacle-constrained null space.

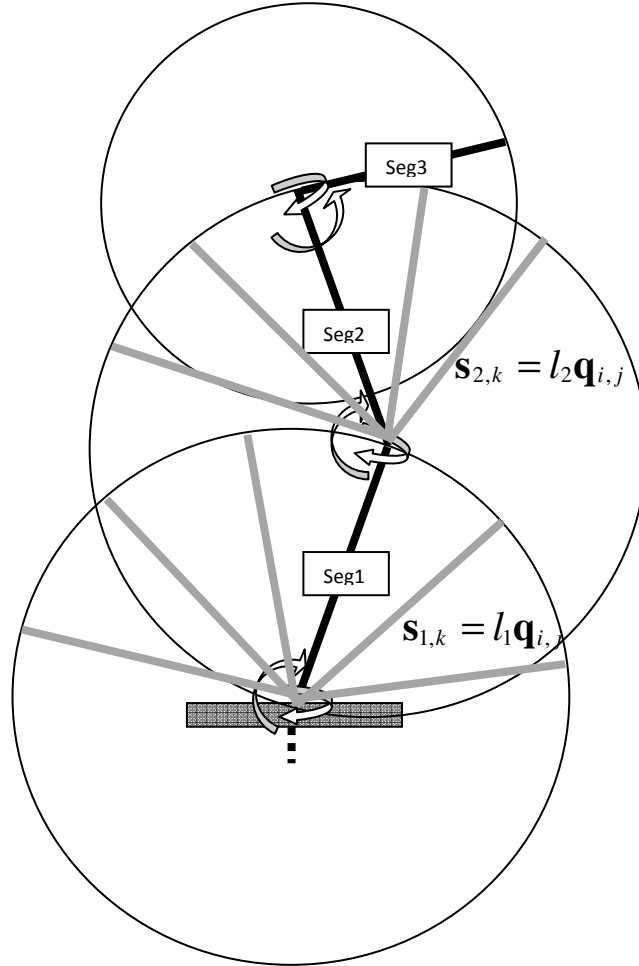


**Fig 2: Segments 1 and 2 quiver generated mappings**

Note in Fig 2 that the third segment is not shown as part of a quiver generated mapping set. This will be explained in the next section.

### **The gap in gMSC**

The selection process for an 8DOF arm will be described. This adds a flexion joint (corresponding approximately to the knuckle) to the standard 7 DOF arms commercially available, and allows IK solution all the way to the angle of attack of a “finger” in a humanoid hand. The path planning step will use 6DOF calculations for efficiency. High DOF arms are necessary for obstacle avoidance in any reasonably complex scenario.

As with conventional MSCs there are forward and backward pathways in the gMSC. However, unlike the conventional form they do not go from end to end. We will define the forward path to originate at the root and the backward path to originate at the target locus. The forward path for 8DOF has only two layers (in old MSC terminology) or stages: those for the first and second segments. The

mappings for these are defined by the quiver, described above. In practice only part of the quiver may be available due to joint angle restrictions (e.g the first segment from the root may for some arm architectures be restricted to the upper hemisphere of the quiver, or less). The backward path originates at the end effector target. It represents the set of permissible angles of attack of the 4<sup>th</sup> segment (end effector or fingers) to the target object. If the application requires a single angle of attack, as in the case of a drill bit, then there is a single vector representing the backward path, but in manipulation tasks there may be a cone of permissible angles. In the latter case, a cone of vectors out of the quiver will constitute the set of available mappings for the 4<sup>th</sup> segment. The backward mappings therefore form either a point, or points on a section of sphere bounded by the permissible cone.

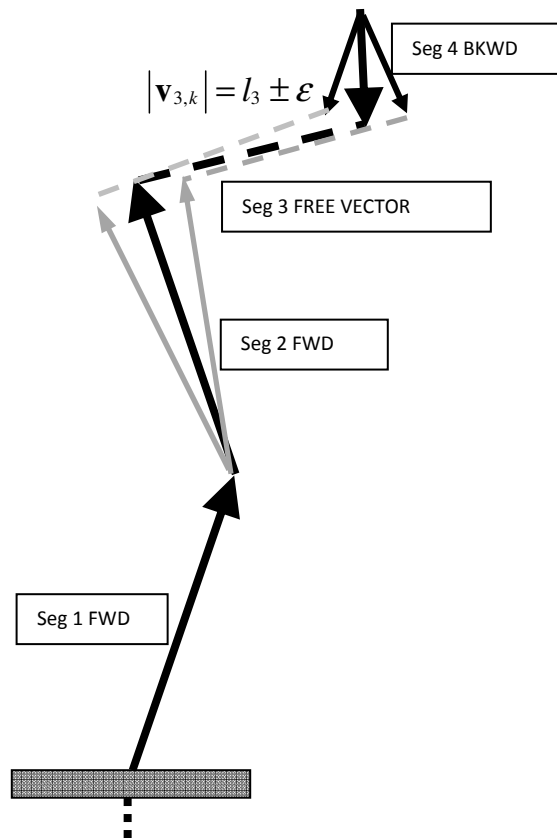


**Fig. 3: gMSC forward and backward (cone) mappings, and free vector in gap.**

Notice that we have not described the mapping set for segment 3. This is the *gap* in the gMSC. It is filled by computing the vector  $\mathbf{v}_{3,k}$  in Fig 3 between the distal end of a segment 2 mapping and some point of the spherical defined by the permissible cone of the 4<sup>th</sup> segment surface (for the moment, consider it to be the center). However, since we are assuming an arm with fixed length segments, only a vector of the physical length of segment 3 is allowable. So we can reject any segment 2 hypothesis whose distal locus requires a vector of the wrong length to span the gap. This is a strong pruning condition. It is most strict when the “cone” of segment 4 contains only a single vector. The

reader is reminded that the segment 3 vectors are not restricted to the directions available in the quiver. It is a “free vector” determined by the endpoints it must satisfy, but its length is fixed.

When the target for segment 3 is bounded by a cone of non-zero diameter, the spatial location of the distal end of the segment 2 mapping is not so critical, as illustrated in Fig 2, since that third segment vector need only find some point on the cone-end surface that satisfies its length constraint. Since the quiver subset inside the cone has relatively few members, the cost of checking against all of these, or a sparse sampling is quite low. A faster initial geometric check based on the angle of incidence of the segment 3 vector to the cone central axis and cone diameter can prune even this search. The “free vector” of segment 3 therefore becomes a strong pruning condition on the distal locii of the segment 2 mappings even when the segment 4 cone has some breadth. In practice we allow a small epsilon in the length of the free vector, either because we don’t require an exact solution, as in path planning, or because we will be able to compute an exact solution at very low cost once we have an good approximation, as will be discussed in the next section.

The “gap” therefore is the primary selection mechanism for viable IK solutions from the sets of segment hypotheses which survive obstacle pruning. Simply, a sequence of non-obstructed segment vectors belongs to the IK solution set  $S_{IK}(\mathbf{r}, \mathbf{t})$  from root  $\mathbf{r}$  to target  $\mathbf{t}$  if the length of the gap vector  $\mathbf{v}$  is of the length  $l$  of the associated arm segment. For a four segment arm:

$$(\mathbf{s}_{1,k1}, \mathbf{s}_{2,k2}, \mathbf{v}_3, \mathbf{s}_{4,k4}) \in S_{IK}(\mathbf{r}, \mathbf{t}) \quad \text{where} \quad (\mathbf{r} + \mathbf{s}_{1,k1} + \mathbf{s}_{2,k2}) - (\mathbf{t} - \mathbf{s}_{4,k4}) = \mathbf{v}_3$$

if

$$abs(|\mathbf{v}_3| - l_3) < \epsilon \quad \text{AND} \quad obs(\mathbf{s}_{1,k1}, \mathbf{s}_{2,k2}, \mathbf{v}_3, \mathbf{s}_{4,k4}) = false$$

### Exact IK solution with discretized segment mappings

As mentioned above, we allow a small range of lengths for the segment 3 vector, because once we have a close solution we can recalculate in a fraction of a microsecond for an exact solution, if required. For a 6DOF solution we use the endpoint of segment 1 as one vertex of a triangle. The target point is the second vertex. And since we know the exact lengths of segment 2 and 3, we have a triangle whose sides are of known length. We also know the plane of the approximate solution which has been cleared for collisions. So the joint angles can be readily calculated for an exact solution despite the fact that the first segment’s endpoint position was discretized. For an 8DOF problem we take the end of the second segment as the triangle vertex and the target position as the second, and do as for 6DOF, but solving for exact joint angles for joints 3 and 4. Again, the discretizations of segments 1 and 2 do not preclude an exact solution.

### Testing for collisions

Before we proceed to the algorithm, it will be useful to have in mind how obstacles are avoided. As alluded to earlier obstacles are represented as voxels of different value than clear space in a 3D grid. When the mapping for a particular segment hypothesis is being tested for viability in the IK solution set, it is first tested to see if it clears all obstacles. The test is simple. The mapping, or segment hypothesis, is represented as a vector of certain length (i.e. the quiver unit vector times the segment length). That vector is marked along its length by  $n$  equi-spaced points. The locus of each of those

points in the general frame space is used to compute indices into the obstacle grid array. If the voxel at that index set is marked as an obstacle the entire segment hypothesis is rejected as having collided with an obstacle. This is a very low cost approach to checking for collision as it involves no search. In practice, the obstacle volumes are dilated to larger dimensions when the obstacle grid array is initialized to accommodate for the thickness of the arm and some degree of clearance margin. The intervals of the test points along the segment vector need only be close enough so that the clearance margin guarantees that the arm could not have collided with the actual, as opposed to dilated, boundaries of the obstacle.

As will be seen later, the division of a segment into test loci for obstacle collision also provides the waypoints for path planning with no extra computation.

### **The procedure for IK solution**

Step 1: All the permissible quiver-generated mappings for segment 1 are tested (a) to determine if the distal end is less than the sum of segment 2 and segment 3 lengths from any of the segment 4 endpoints (or from waypoints during path planning), and (b) for collisions. Only the survivors are marked as viable and saved as a dense set. This step can be done in parallel.

Step 2a: For each viable mapping in the survivor set for segment 1, all the quiver-generated segment 2 mappings from each segment 1 distal locus are checked for obstacle collision.

Step 2b: For any survivor from Step 2a the distal endpoint is checked for viability across the gap to the 4<sup>th</sup> segment backward mapping endpoints as described above and illustrated in Fig 2. If a viable spanning vector is found, it too is checked for obstacle collisions, in the same manner as the mapped segments. Any which survive all the pruning conditions constitute a four segment chain which is a viable IK solution.

Step 3: All survivors are captured, and one is chosen as the “reach pose” IK solution. If for some reason, a viable path to this pose cannot be found, as will be discussed below, another reach pose solution from the survivor set may be chosen.

Steps 2a and 2b can be parallelized in various ways. For GPGPUs the practical deployment is to create as many threads as there are vectors in the mapping set for segment 2. Each thread computes one segment 2 mapping for all the surviving segment 1 hypotheses from Step 1, and tests those for collision and completion across the gap. Each thread stores any viable solutions it finds.

If this process seems very simple, that is because it is. It is an illustration of the benefit of choosing a well suited representation for solving a problem by computation.

### **Path Planning**

The original insight of using MSC as a path planner in the presence of terrain advantages and obstacles was published in [2]. The use of the same path planning process as the guidance for multilink robot was published in [3]. Those examples used linkages of many segments to snake through complex terrain, but in two dimensions. Here we use the same principle in three dimensions, but exploit the reach pose IK solution to provide an obstacle avoiding path from the arm root to the



target locus. This path will be used for some joint of the arm to follow, and provide a sequence of IK target locations or waypoints to determine a smooth sequence of obstacle avoiding poses which take the arm from its initial folded pose to the reach pose.

We could make these computations for the 8DOF arm, moving the distal end of the 4<sup>th</sup> segment along the path defined by the reach pose. But on the assumption that the 4<sup>th</sup> segment is short, we instead move the 3<sup>rd</sup> segment distal end along the path via a sequence of 6DOF IK solutions and keep the 4<sup>th</sup> segment out of harm's way by aligning it with the reach pose defined path.

We also exploit the previous computation of  $n$  waypoints along each segment as part of the collision testing. The same  $n$  points along each segment vector that were tested for collision and survive that test, make ideal waypoints for the path planning stage. All that needs to happen to set this up is for the collision test points to be saved temporarily in an array, and then if the 4 segments survive all tests, for those waypoints to be saved in an array associated with the IK solution. There is virtually no extra cost.

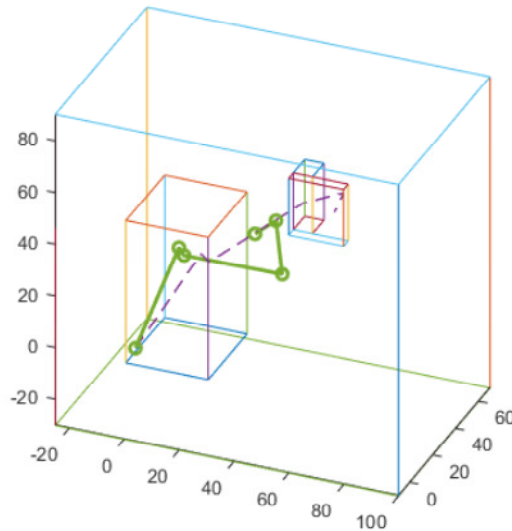


**Fig 4: Midpath Waypoint IK Solution**

Fig 4 illustrates an obstacle-clearing IK solution for a midpath waypoint along the lengths of the reach pose shown in Fig 1.

At the last step of the reach pose phase, when an IK solution amongst the surviving set is chosen, the waypoint set associated with it is also selected.

### **Smooth sequence computation**

The objective in path planning is that the sequence of arm poses from the initial folded pose to the final reach pose form a sequence yielding smooth continuous arm motion. At the same time, we do

not need the precision of endpoint placement we require for the reach pose. So we can allow a greater epsilon in putting the endpoint (either 3<sup>rd</sup> or 4<sup>th</sup>) near the waypoints, but apply some strong criteria so assure that each successive pose along the path is a smooth and nearby transition from the previous.

The most constraining pose is the reach pose. That is, the path pose nearest the reach pose must be a close relative, so the transition from next to last to last does not require big motions. We will see how the other end takes care of itself: one of the nice regularities in this solution to the problem.

Since the reach pose is the most constraining, it makes sense to work backward along the waypoints finding the set of IK solutions at each successive waypoint which are closest in configuration to the previously found one. To enforce this consistency we apply a set of filters based on the previously found pose. This filtering step will be described below.

A backward sequence of poses is thus captured which, normally, will constitute a smooth path. There are edge cases which don't satisfy the smoothness condition, or may not complete the path at all. But these only occur in highly congested areas which don't allow the arm to fold as needed to follow the path at some point. We will discuss this later.

The next interesting case arises at the waypoint that coincides with the root locus. If we have been using 6DOF solutions, then the distal end of the 3<sup>rd</sup> segment must be co-located with the root regardless of the backward sequence which took us there. Hence the three segments form a triangle and define a plane (Fig 5). That pose is not the start position of the arm. The arm starting pose is assumed to be folded zig-zag on itself, all segments in a plane (Fig 6).

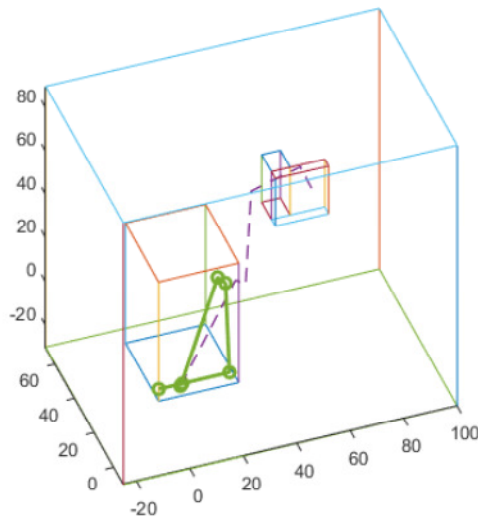


**Fig 5: Root Waypoint IK Solution**

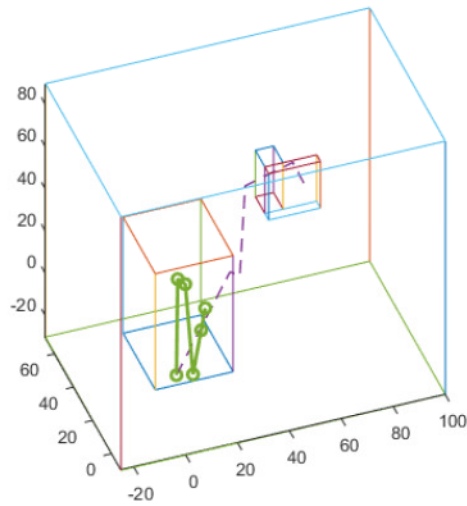


**Fig 6: Initial Folded Arm Pose**

That plane is likely not to be the same plane as the triangle of the root waypoint, but it is a simple matter to rotate the folded pose into the same plane as the root waypoint triangle pose. It requires only rotation of the root joint so that 1<sup>st</sup> segment of the fold pose co-aligns with the 1<sup>st</sup> segment of the root waypoint triangle pose. Now it is a simple matter to unfold the remaining segments from their fold position to the root waypoint pose by angle interpolation. That sequence, reversed completes the backward sequence from reach pose to folded initial pose.

Now executing that whole sequence in forward order constitutes a smooth motion sequence, clearing all obstacles, from initial pose to reach pose

### **Filtering for smoothness**

As each IK solution survives both obstacles and completion within a prescribed epsilon of the waypoint it is checked to determine if it is a smooth transition from the previous waypoint solution. There are several tests that work successfully. (a) The distance from the locus of each joint from its corresponding joint in the previous solution must be less than a certain distance approximating to the distance between the waypoints. This is done for joints 1 and 2. When segments 1 and 2 are much longer than segment 3, joint 1 will generally move about half the distance between waypoints along the direction of the waypoints and joint 2 will move about the distance between waypoints. Restricting the allowable motion to approximately these amounts, plus some slack, will prevent dramatic rotations of the solution around the waypoint path. This is a nice geometric regularity that can be exploited with very little cost. Another criterion that can be substituted or added is the change in angle of segment 1 and 2 at each waypoint step, though the distance criterion alone appears to produce smooth motion along the path in all cases tested so far.

There is, however, a caveat regarding the smoothness filtering. When the path makes a large angular turn, the obstruction configuration can require that the pose sequence does in fact require a large rotation as it crosses this turn. If the filtering is set to maximize smoothness in more normal path and

obstacle configurations, it can reject a pose solution which effectively turns the corner, but requires a rotation which is precluded. Fig 8, below is an example, though it is not visible in the frames presented. This circumstance requires that the filter criteria be relaxed for the poses that cross the turn of the path. This adjustment is best done adaptively (i.e. after failure to find a pose solution at a given waypoint), because the conditions which require it are hard to categorize and detect in advance. The time penalty for this adaptation is very small: a few milliseconds on large GPU.

Another regularity that may provide speedup in non-parallel implementations is that the geometrically similar solutions tend to cluster nearby in the sequence of computation, so during path planning one need only test mapping indices near those from the previous waypoint to find a smoothly connecting solution for the next waypoint. (This optimization does not appear to provide much benefit in parallel implementations, probably because it increases thread divergence.)

### Other Examples

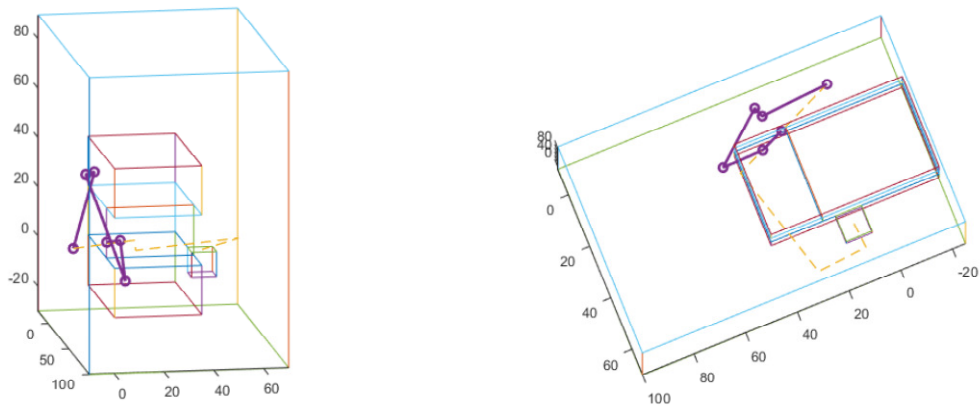


Fig 7a: Early Path

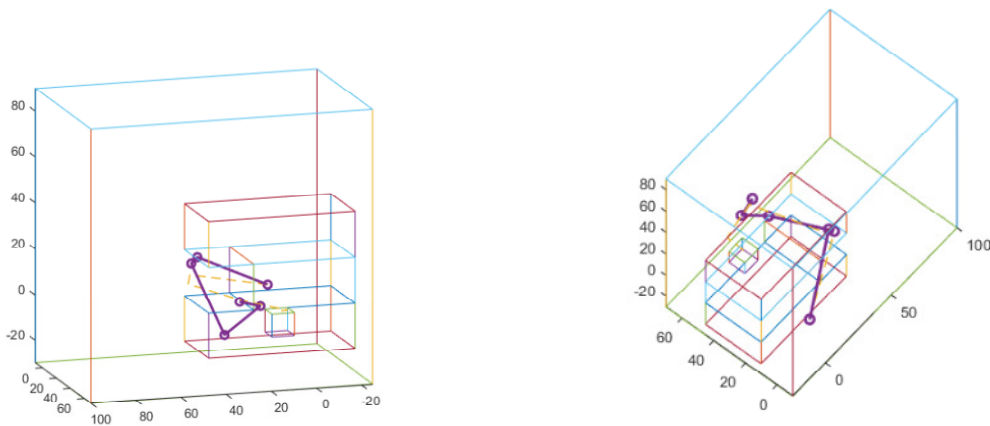
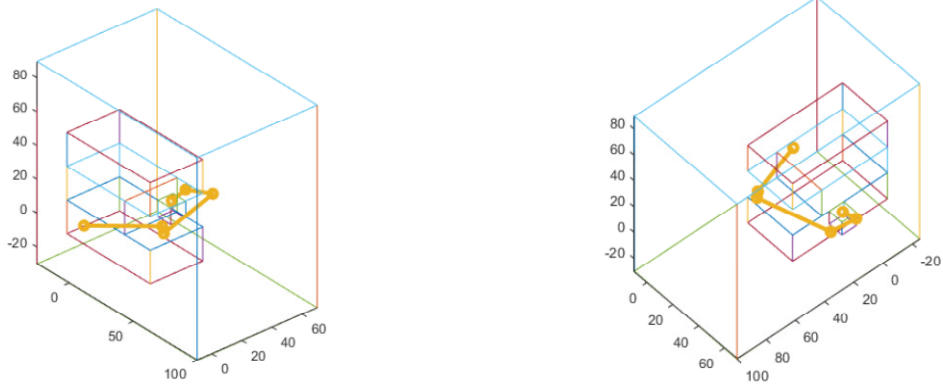
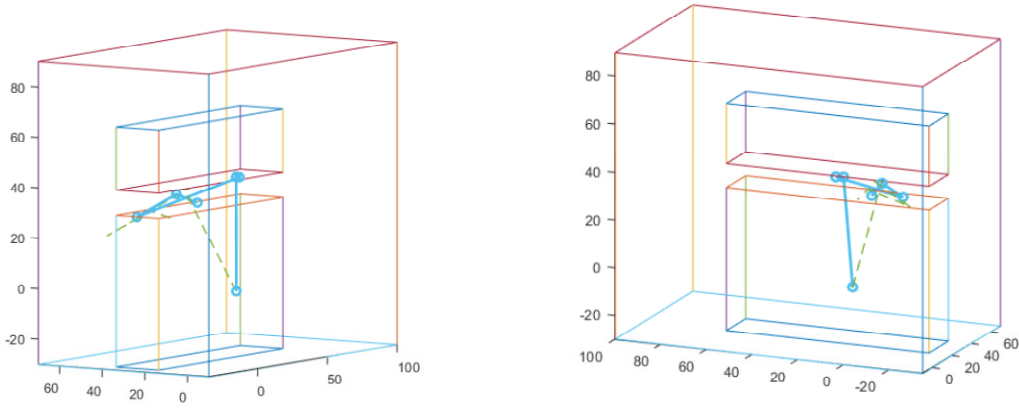


Fig 7b: Mid Path



**Fig 7c: Reach Pose, End Path**



**Fig 8a: Early Path**

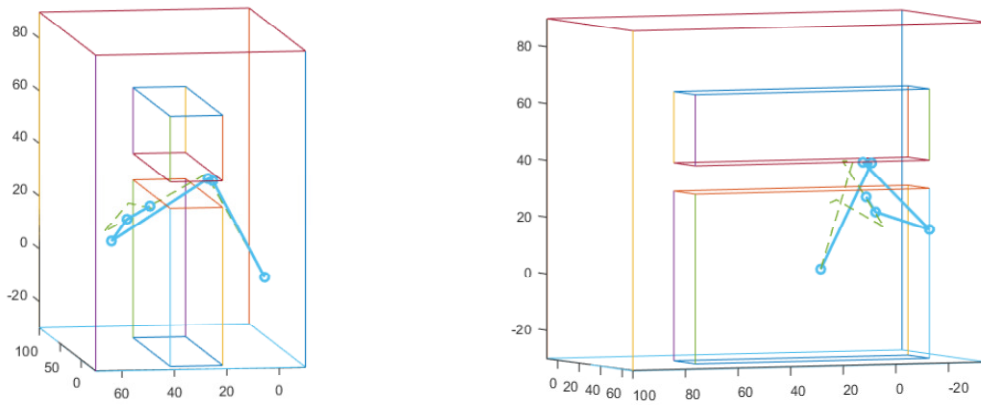


**Fig 8b: Mid Path**

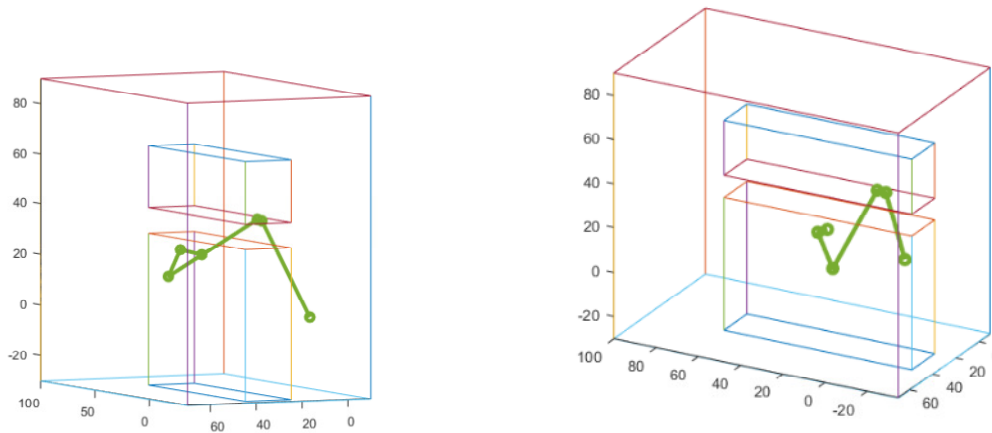


**Fig 8c: Reach Pose, End Path**

### Edge and pathological cases

The method for computing arm IK solutions in the presence of obstacles should always find a reach pose if the architecture of the arm and the configuration of obstacles allows. Nevertheless, having a reach pose and therefore an obstacle free path for some joint of the arm, does not mean that there is always a corresponding motion plan. One can readily imagine a configuration of obstacles that would preclude any sequence of articulations from pushing a selected joint along the reach pose defined path. A simple example is a narrow tube around the first or second segments.

Therefore, the method for path planning described so far, while probably widely usable in many circumstances, may not work for some. Either there may be no solution by any means, or there may be viable path plans which cannot be arrived at by the method above.

While a systematic approach to these edge cases is part of the work that lies ahead, a few methods suggest themselves.

- 1) A different reach pose in the initial set may be tried as the path.
- 2) The same path is used, but following it is relaxed. Most likely the early part of the backward solution of waypoint poses will succeed due to similarity to the reach pose. But some waypoint along the sequence will not produce a solution because obstacles will kill all poses that reach to or very near the waypoint. Then...
  - (a) An incremental relaxation of the smoothness filtering and the gap epsilon may allow a solution still reasonably close to the waypoint at the expense of motion smoothness. This procedure may allow a stretch of the reach-pose-guided path to be bypassed until it can be rejoined a number of waypoints down the road.

(b) A cloud of target points around the original path may be generated and used as targets, much as described for the segment 4 cone. As solutions are found the cloud would be advanced down the original path.

Method (a) has been tested informally and does work at least for limited constrictions. To date, method (b) has not been tested.

Several more “informed” methods have been considered, and those will be among the tasks for work ahead.

### **Offset Joints and Other Arm Architecture Features**

Figs 3 through 8 depict arms with an offset at joint 2. These were included to demonstrate that the method is not restricted to “coaxial” arm architectures, though the latter is used for description of the method. The offset joint shown rotates in azimuth around the axis of the segment and displaces the elevation rotation at some distance from the segment axis. The implementation of this is straightforward and involves a single rotation matrix. Further discussion is not appropriate to a presentation of this nature but may be discussed in some detail in a later, more technical presentation. As many joints may be offset as desired, at a small cost in extra computation, approximately 50-80 msec per joint for the whole reach pose and path planning process on a large GPU, although newer GPUs with exposed hardware 4x4 matrix multipliers may reduce this overhead to effectively naught.

As noted earlier, prismatic joints may be included. The mappings in this case are changes in length of the segment which includes the joint. As with angles, the lengths must be discretized if the prismatic joint is in the first two or last segments. The free vector third segment, of course, implements this without cost.

### **Implementation Performance To Date**

The implementation which generated the examples above is written in C and CUDA (for the GPU executed sections). The first segment computations are done sequentially on the CPU and coded in C. The remaining segment computations are executed in parallel as described earlier on the GPU and are written in CUDA C. 8 waypoints per segment are checked for collision with obstacles, and later used for path planning waypoint computations. On a high-end (200+ watt) Nvidia Quadro GPU the entire computation from start to path plan takes about 200msec for a coaxial arm and about 250msec for a single offset joint arm, as shown in the Figs. The same code takes about a second on a low end (45 watt) Nvidia Quadro GPU. The locality-exploiting optimizations described above for serial hardware implementation have not been tested, since the code diverged from all-serial implementation early in development.

### **Joint Dynamics**

There has been no description of how joint angle velocities are computed in the above scenario. This is a solved problem and will be addressed in a more technical presentation. In summary, however, the joint angle differences between waypoint IK solutions are linearly interpolated to produce smaller

joint angle deltas between sub-waypoints. For each interpolated step, the largest joint angle delta among the 3 or 4 joints becomes the velocity reference. That is, the joint angular velocity is set to produce constant angular change for the joint with the largest delta. The joint angular velocities for the remaining joints are then scaled by the ratio of each one's angular delta to the delta of the largest. This assures that all joints arrive at each interpolated sub-waypoint at the same time. A further refinement guarantees that there is no deceleration at the goal angle for arm actuators which can be instructed to move toward goal angles at specified angular velocities and then decelerate and stop at the goal angle. That refinement is based on replacing goal angles provided to the actuators with a more advanced goal angle before the automatic deceleration of the actuator commences. This strategy has been tested and works well to produce fluid, natural motion, for example in insect locomotion emulation by robot hexapod.

## References

[1] Arathorn D (2002) *Map-Seeking Circuits in Visual Cognition: A Computational Mechanism for Biological and Machine Vision*. Stanford University Press, Stanford, CA, USA.

[2] Arathorn D, (2004), *From Wolves Hunting Elk to Rubik's Cubes: Are the Cortices Composition/Decomposition Engines?*, AAI Symposium on Compositional Connectionism.

[3] Snider RK, Arathorn D, (2006) *Terrain discovery and navigation of a multi-articulated linear robot using map-seeking circuits*. Proc. SPIE 6229, Intelligent Computing: Theory and Applications IV, 62290H (9 May 2006).

Further MSC references and tutorials can be found at [www.giclab.com](http://www.giclab.com)

A video of the path plan execution for the examples in the text can also be found in the References/Technical Reports section of [www.giclab.com](http://www.giclab.com)